Published by :
http://www.ijert.org

International Journal of Engineering Research & Technology (IJERT)
ISSN: 2278-0181
Vol. 8 Issue 05, May-2019

Modeling and Design of UAV with LQG and H_∞ Controllers

Ancy G. Varghese
Electrical and Electronics Engineering
Lourdes Matha College of Science and Technology
Trivananthapuram, India

Sreekala Devi K.
Electrical and Electronics Engineering
Lourdes Matha College of Science and Technology
Trivananthapuram, India

***Abstract*— Autonomous flying robots, also known as unmanned aerial vehicles (UAVs) or "drones" have been developed and widely used for purposeful civilian and military applications. Control of UAVs with a view to minimize disturbance, therefore is a major area of research in control systems. In this paper the multi-input, multi-output under-actuated linear model configuration is deduced by aerodynamic analysis. The model of Dryden turbulence is used as one of the major disturbances affecting the UAVs and then dynamic output feedback robust controller is synthesized. Two robust controllers which are readily applicable to problems involving multivariable systems are designed and compared. The aim of these controllers is to achieve robust stability margins and good performance in system. LQG method is a systematic design approach based on shaping and recovering open-loop singular values while mixed-sensitivity H_∞ method is established by defining appropriate weighting functions to achieve good performance and robustness. Simulation results of the two controllers are compared.**

Keywords*— *Unmanned aerial vehicle (UAV), Dryden turbulence, H_∞ Controller, LQG Controller

I. INTRODUCTION

Unmanned Aerial Vehicles (UAVs) form an area of intensive research in the field of control systems today. The multitude of applications of UAVs in a range of fields such as agriculture, aerial photography, search and rescue operations, product delivery and surveillance make them the favorite alternative to the conventional aircrafts, especially in situations where manned vehicles are dangerous. The introduction part of the papers [1] and [2] describe the various applications to which UAVs are put to. Being a multi-input multi-output (MIMO), under actuated, unstable and highly coupled system, their control and operation are highly challenging. Therefore research concentrating on the control of UAVs becomes very much relevant today. PID, LQR/G, SMC, Integrator Backstepping, Adaptive control algorithms, Robust Control algorithms, and Optimal control algorithms including the H_∞ are the ones that are tested and used for the control of UAVs. In this study it is attempted to make an evaluation of the comparative performance of the two linear robust controllers namely LQG and H_∞ controllers.

The design and comparison of LQG/LTR and H_∞ controllers for a VSTOL flight control system are dealt with in [3]. Robust Control of UAVs using H_∞ Control Paradigm is discussed in [4]. A study by Yenal Vural and Chingiz Hajiyev describes the design of an altitude control system for a small UAV using classical control methods, optimal control methods and fuzzy logic [5]. The technique of designing and implementing a non-linear robust controller to regulate an UAV quadrotor are described by Ortiz and others [6]. A discussion on the application of Polynomial LQG and Sliding Mode Observer for a Quadrotor UAV is given in [7].

This paper describes the dynamic model of UAV and then describes the design of the two controllers. The performance of each controller designed is then tested and compared.

II. DYNAMIC MODEL OF UAV

The dynamic model of UAV used for this study is a linearized state-space model derived from a six-degree-of-freedom nonlinear model of a typical general aviation aircraft. This particular flight dynamics model is chosen mainly because of the well-behaved open-loop dynamics of the aircraft and the similarity in handling characteristics of small and medium-scale UAVs. The model treats the aircraft as a rigid body and includes the following 12 states:

$$X= \{u, v, w, p, q, r, \phi, \psi, X_N, Y_E, h\}^T$$

where, {u, v, w} denote the body-referenced translational velocity components, {p, q, r} represent the body-referenced angular velocity components, $\{\phi, \theta, \psi\}$ are the roll, pitch, and yaw angles, and $\{X_N, Y_E, h\}$ denote the inertial (north, east, altitude) position. The UAV model includes the following control inputs:

$$U= \{\delta_e, \delta_T, \delta_a, \delta_r\}^T$$

where, δ_e is the elevator deflection, δ_T represents the thrust control, δ_a is the aileron deflection, and δ_r is the rudder deflection.

The nonlinear aircraft model was linearized about a wing-level constant-altitude trim condition corresponding to

$X^*= \{u^*, v^*, w^*, p^*, q^*, r^*, \varphi^*, \theta^*, \psi^*, X^*_N, Y^*_E, h^*\}^T$
$=\{176.4$ ft⁄s, 0, −0.244 ft⁄s, 0, 0, 0, 0, 0.08 deg, 0, 0, 0, $0\}^T$

International Journal of Engineering Research & Technology (IJERT)
ISSN: 2278-0181
Vol. 8 Issue 05, May-2019

This trim condition corresponds to a sea level altitude with the aircraft close to a zero angle of attack. The trim control inputs are:

$U=\{\delta^*_e, \delta^*_T, \delta^*_a, \delta^*_r\}^T$
$=\{0.0573 \text{ deg}, 0.5406, 0, 0\}^T$

The linearization process yields decoupled longitudinal and lateral state-space models of the following form:

$X_{long} = A_{long}X_{long} + B_{long}U_{long}$
$X_{lat} = A_{lat}X_{lat} + B_{lat}U_{lat}$

where X and U represent changes in the state and control variables from the trim state. These vectors are defined as follows:

$X_{long} = \{u, w, q, \theta, h\}^T$
$U_{long} = \{\delta_e, \delta_T\}^T$
$X_{lat} = \{v, p, r, \phi, \psi\}^T$
$U_{lat} = \{\delta_a, \delta_r\}^T$

The specific longitudinal and lateral linear models are then given by

$$\begin{bmatrix}\dot{v}\\ \dot{p}\\ \dot{r}\\ \dot{\phi}\\ \dot{\psi}\end{bmatrix} = \begin{bmatrix}-0.2771 & -0.244 & -176.4 & 32.2 & 0\\ -0.091 & -8.4174 & 2.1967 & 0 & 0\\ 0.0261 & -0.3535 & -0.7684 & 0 & 0\\ 0 & 1 & -0.0014 & 0 & 0\\ 0 & 0 & 1 & 0 & 0\end{bmatrix}\begin{bmatrix}v\\ p\\ r\\ \phi\\ \psi\end{bmatrix} + \begin{bmatrix}0 & 12.5086\\ -29.0588 & 23.2037\\ -0.2273 & -4.6752\\ 0 & 0\\ 0 & 0\end{bmatrix}\begin{bmatrix}\delta_a\\ \delta_r\end{bmatrix} \quad (1)$$

$$\begin{bmatrix}\beta\\ p\\ r\\ \phi\\ \psi\end{bmatrix} = \begin{bmatrix}0.005669 & 0 & 0 & 0 & 0\\ 0 & 1 & 0 & 0 & 0\\ 0 & 0 & 1 & 0 & 0\\ 0 & 0 & 0 & 1 & 0\\ 0 & 0 & 0 & 0 & 1\end{bmatrix}\begin{bmatrix}v\\ p\\ r\\ \phi\\ \psi\end{bmatrix} + \begin{bmatrix}0 & 0\\ 0 & 0\\ 0 & 0\\ 0 & 0\\ 0 & 0\end{bmatrix}\begin{bmatrix}\delta_a\\ \delta_r\end{bmatrix} \quad (2)$$

$$\begin{bmatrix}\dot{u}\\ \dot{w}\\ \dot{q}\\ \dot{\theta}\\ \dot{h}\end{bmatrix} = \begin{bmatrix}-0.0676 & 0.0308 & 0.2373 & -32.2 & 0\\ -0.3679 & -2.0273 & 171.5 & 0.0445 & 0\\ 0 & -0.0501 & -2.0804 & 0 & 0\\ 0 & 0 & 1 & 0 & 0\\ -0.0014 & -1 & 0 & 176.4 & 0\end{bmatrix}\begin{bmatrix}u\\ w\\ q\\ \theta\\ h\end{bmatrix} + \begin{bmatrix}-0.0391 & 7.3017\\ -28.2839 & 0\\ -11.9328 & 0\\ 0 & 0\\ 0 & 0\end{bmatrix}\begin{bmatrix}\delta_e\\ \delta_t\end{bmatrix} \quad (3)$$

$$\begin{bmatrix}V_a\\ \alpha\\ q\\ \theta\\ h\end{bmatrix} = \begin{bmatrix}0.9999 & -0.00138 & 0 & 0 & 0\\ 7.84\times10^{-6} & 0.00567 & 0 & 0 & 0\\ 0 & 0 & 1 & 0 & 0\\ 0 & 0 & 0 & 1 & 0\\ 0 & 0 & 0 & 0 & 1\end{bmatrix}\begin{bmatrix}u\\ w\\ q\\ \theta\\ h\end{bmatrix} + \begin{bmatrix}0 & 0\\ 0 & 0\\ 0 & 0\\ 0 & 0\\ 0 & 0\end{bmatrix}\begin{bmatrix}\delta_e\\ \delta_t\end{bmatrix} \quad (4)$$

III. CONTROLLER DESIGN

A. *LQG Controller*

The block diagram of an LQG Controller is shown in fig. 1.

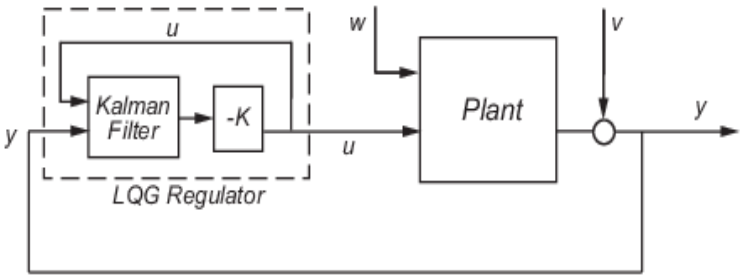

Fig. 1. Block diagram of an LQG Controller

The linear-quadratic-Gaussian (LQG) control problem is a basic and fundamental optimal control in control theory. The LQG controller consists of a Kalman filter, i.e. a linear-quadratic estimator (LQE), coupled with a linear-quadratic regulator (LQR). Applying the separation principle, the two can be designed and computed independently. Consider the plant in state space form,

$$\dot{x} = Ax + Bu + w \quad (5)$$
$$Y = Cx + Du + v \quad (6)$$

where, w is the random noise disturbance input (process noise) and v the random measurement (sensor) noise.

Controller is given by,

$$u=-K\hat{x} \quad (7)$$

where K is the controller gain, $K=R^{-1}B^TP$

and $\hat{x}$ is the state estimator. P is the positive definite solution of algebraic riccati equation

$$A^TP+PA-PBR^{-1}B^TP+Q=0 \quad (8)$$

The optimal observer known as Kalman filter is given by,

$$\dot{\hat{x}}=A\hat{x}+Bu+L(y-C\hat{x}) \quad (9)$$

where, L is the estimator gain, $L=SC^TR_0^{-1}$
and S is the positive semi-definite solution of algebraic riccati equation

$$AS+SA^T-SC^TR_0^{-1}CS+Q_0=0 \quad (10)$$

International Journal of Engineering Research & Technology (IJERT)
ISSN: 2278-0181
Vol. 8 Issue 05, May-2019

Q_0 and R_0 are Co-varience matrices which represent the intensity of the process and sensor noise inputs.

B. H_∞ CONTROLLER

Fig. 2 shows the block diagram of an H_∞ controller.

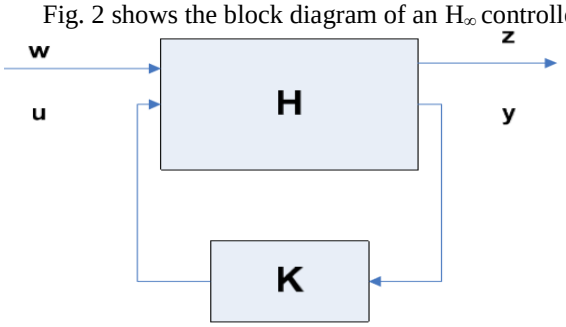

Fig. 2. Block diagram of H_∞ Controller

The plant section has two inputs and two outputs. The plant inputs are control inputs, u and exogenous inputs, w. The plant can be represented in state-space form as:

$$\dot{x} = Ax + B_1 w + B_2 u \quad (11)$$

$$z = C_1 x + D_{11} w + D_{12} u \quad (12)$$

$$y = C_2 x + D_{21} w + D_{22} u \quad (13)$$

To solve the control problem certain assumptions have to be satisfied. They are

- The pair (A, B_2) is stabilizable and (C_2, A) is detectable.
- Rank D_{12}=dim u , rank D_{21}=dim y
- Rank $\begin{bmatrix} A - j\omega I & B_2 \\ C_1 & D_{12} \end{bmatrix}$ =n+m_2 for all frequencies
- Rank $\begin{bmatrix} A - j\omega I & B_1 \\ C_2 & D_{21} \end{bmatrix}$ =n+p_2 for all frequencies
- D_{11}=0 and D_{22}=0

The controller gain Kc is given by,

$$u = -K_c \hat{x} \quad (14)$$

State estimator is given by

$$\dot{\hat{x}} = A\hat{x} + B_2 u + B_1 \hat{w} + Z_\infty K_e (y - \hat{y}) \quad (15)$$

where,

$$\hat{w} = \gamma^{-2} B_1' X_\infty \hat{x} \quad (16)$$

$$\hat{y} = C_2 \hat{x} + \gamma^{-2} D_{21} B_1' X_\infty \hat{x} \quad (17)$$

$$Z_\infty = (I - \gamma^{-2} Y_\infty X_\infty)^{-1} \quad (18)$$

$$K_c = \widetilde{D_{12}} (B_2' X_\infty + D_{12}' C_1) \quad (19)$$

$$\widetilde{D_{12}} = (D_{12}' D_{12})^{-1} \quad (20)$$

$$K_e = (Y_\infty C_2' + B_1 D_{21}') \widetilde{D_{21}} \quad (21)$$

$$\widetilde{D_{21}} = (D_{21} D_{21}')^{-1} \quad (22)$$

X_∞ and Y_∞ are solutions to the controller and estimator Riccati equations:

$$X_\infty = \mathrm{Ric}\begin{bmatrix} (A - B_2 \widetilde{D_{12}} D_{12}' C_1) & \gamma^{-2} B_1 B_1' - B_2 \widetilde{D_{12}} B_2' \\ -\widetilde{C_1}' \widetilde{C_1} & -(A - B_2 \widetilde{D}_{12} D_{12}' C_1)' \end{bmatrix} \quad (23)$$

$$Y_\infty = \mathrm{Ric}\begin{bmatrix} (A - B_1 D_{21}' \widetilde{D_{21}} C_2)' & \gamma^{-2} C_1' C_1 - C_2' \widetilde{D_{21}} C_2 \\ -\widetilde{B_1} \widetilde{B_1}' & -(A - B_1 D_{21}' \widetilde{D}_{21} C_2) \end{bmatrix} \quad (24)$$

IV. RESULTS AND DISCUSSIONS

Figures 3 and 4 show the plot of the uncompensated lateral and longitudinal systems respectively. The output of the controlled lateral system with LQG and H_∞ Controllers respectively are given in figs 5 and 6. The controlled longitudinal system outputs are as in figs. 7 and 8.

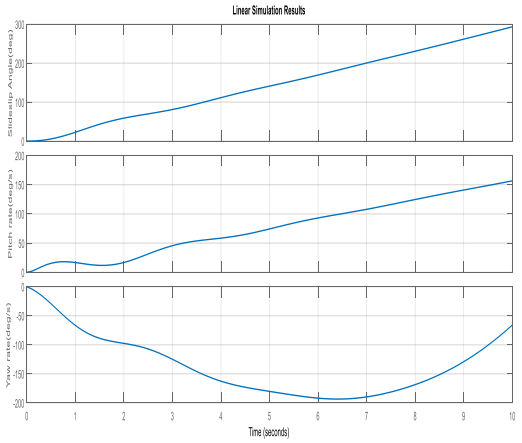

Fig. 3. Uncompensated Lateral System

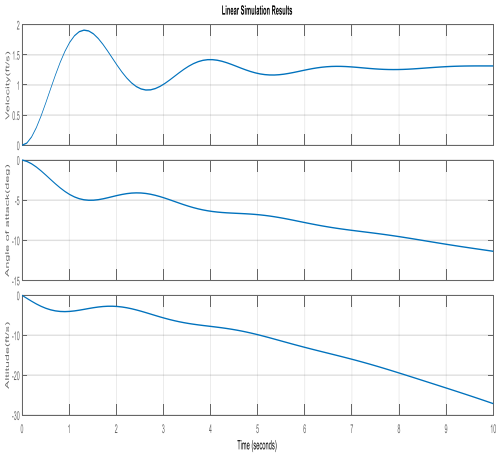

Fig. 4. Uncompensated Longitudinal System

International Journal of Engineering Research & Technology (IJERT)
ISSN: 2278-0181
Vol. 8 Issue 05, May-2019

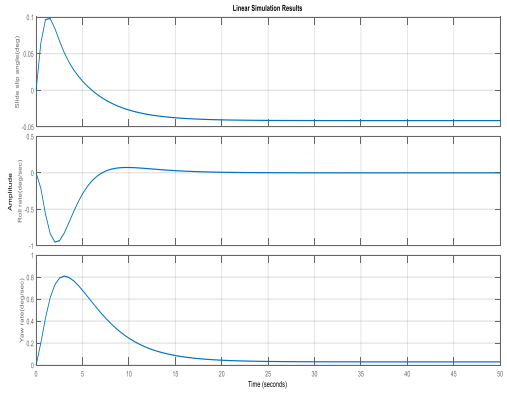

Fig. 5. Lateral System with LQG Controller

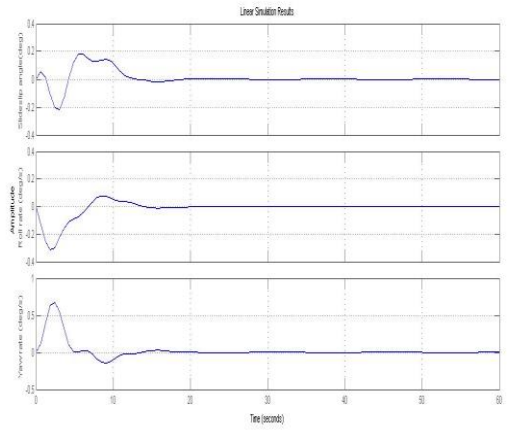

Fig. 6. Lateral System with H∞ Controller

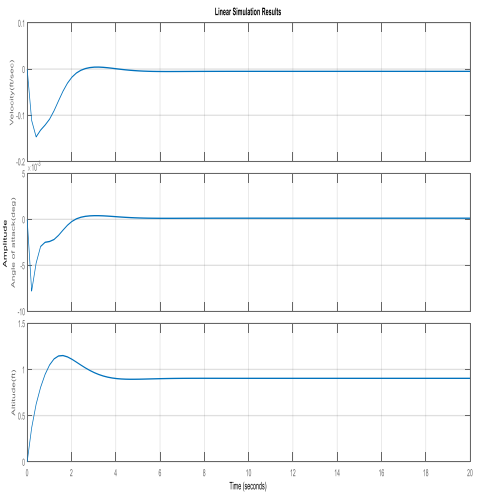

Fig. 7. Longitudinal System with LQG Controller

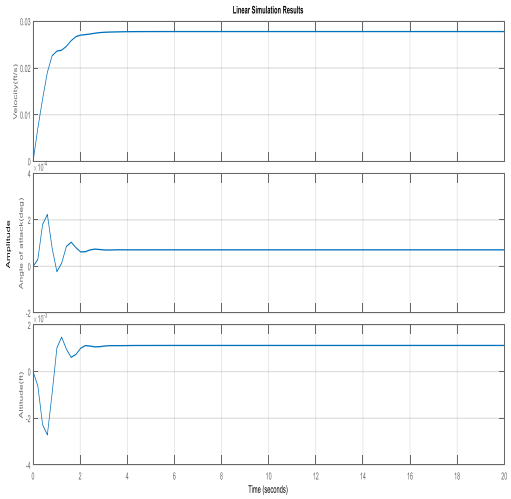

Fig. 8. Longitudinal System with H∞ Controller

Comparison of the outputs with respect to the two controllers used in the study is as given in tables I and II.

TABLE I. COMPARISON - LATERAL

Lateral		***LQG Controller***	***H∞ Controller***
Slideslip angle	Peak overshoot	0.1	0.1
	Settling time	15	13.7
Roll rate	Peak overshoot	0.1	0.07
	Settling time	17.5	14.4
Yaw rate	Peak overshoot	0.8	0.6
	Settling time	21.5	18.1

TABLE II. COMPARISON - LONGITUDINAL

Longitudinal		***LQG Controller***	***H∞ Controller***
Velocity	Peak overshoot	0.09	0.028
	Settling time	4.2	2.2
Angle of attack	Peak overshoot	0.1	0.00022
	Settling time	4.8	2.5
Altitude	Peak overshoot	0.8	0.005
	Settling time	4.3	3

V. CONCLUSION

Comparison of the data in the two tables leads to the conclusion that performance of the H∞ Controller is better when compared to the LQG system.

International Journal of Engineering Research & Technology (IJERT)
ISSN: 2278-0181
Vol. 8 Issue 05, May-2019

REFERENCES

[1] López, J., R. Dormido, S. Dormido, and J. P. Gómez, "A Robust Controller for an UAV Flight Control System," The Scientific World Journal, 2015 .

[2] Nirmit Prabhakar, Andrew Painter, Richard Prazenica, and Mark Balas "Trajectory-Driven Adaptive Control of Autonomous Unmanned Aerial Vehicles with Disturbance Accommodation". JOURNAL OF GUIDANCE,CONTROL, AND DYNAMICS, 2018

[3] Zarei, Jafar; Montazeri, Allahyar; Motlagh, Mohmmad Reza Jahed; Poshtan, Javad. "Design and comparison of LQG/LTR and H-infinity controllers for a VSTOL flight control system" Journal of The Franklin Institute, Vol. 344, No. 5 pp. 577-594.

[4] M. Z. Babar, S. U. Ali, M. Z. Shah, R. Samar, A. I. Bhatti and W. Afzal. "Robust Control of UAVs using Hœ Control Paradigm". IEEE 9th International Conference on Emerging Technologies, 2013

[5] S. Yenal Vural and Chingiz Hajiyev. "A comparison of longitudinal controllers for autonomous UAV". Int. J. Sustainable Aviation, Vol. 1, No. 1, 2014 . Pp 58-71

[6] J. P. Ortiz, L. I. Minchala, and M. J. Reinoso. "Nonlinear Robust H-Infinity PID Controller for the Multivariable System Quadrotor". IEEE Latin America Trans., 14, 3, March 2016. Pp. 1176 – 1183

[7] Abdellah Mokhtari, Abdelaziz Benallegue, and Abdelkader Belaidi. "Polynomial Linear Quadratic Gaussian and Sliding Mode Observer for a Quadrotor Unmanned Aerial Vehicle". *J. Robot. Mechatron.*, Vol.17, No.4, pp. 483-495, 2005.

.